ANL-HEP-PR-77-38

The Diffractive Process in Six-Prong Proton-Proton Interactions at 205 GeV/c*

M. DERRICK, B. MUSGRAVE, P. SCHREINER, P. F. SCHULTZ, M. SZCZEKOWSKI†, and H. YUTA‡

Argonne National Laboratory, Argonne, Illinois 60439

We have studied the 6-prong events in a 50,000 picture exposure of the Fermilab 30-inch HBC to a 205 GeV/c proton beam. The data consist of complete measurements of 442 events, each containing a proton track with $P_{Lab} < 1.4$ GeV/c. A low mass diffractive peak is seen in the events with 5 charged particles in the forward center-of-mass hemisphere. An analysis based on the rapidity distributions of the outgoing tracks and the missing mass gives a single diffractive cross section of 0.88 ± 0.12 mb for both hemispheres of which the final state $pp\pi^+\pi^+\pi^-\pi^-$ contributes 0.18 ± 0.07 mb. In the diffractive sample, only 0.20 ± 0.06 mb corresponds to events decaying through an intermediate state containing a Δ^{++}. We measure an upper limit for the double diffraction cross section of 0.38 ± 0.12 mb.

---

*Work supported by the U.S. Energy Research and Development Administration.

†On leave of absence from the Institute for Nuclear Research, Warsaw, Poland.

‡Present Address: Tohoku University, Sendai 980, Japan.

Studies of the inclusive proton reaction

$$p + p \rightarrow p + X \qquad (1)$$

have been made over a wide range of energies.[1] The data show a low mass peak in the mass squared distribution for X (MM^2). In our experiment at 205 GeV/c in the 30-inch hydrogen bubble chamber at the Fermi National Accelerator Laboratory, it was found that only the low multiplicity events (2-, 4-, and 6-prongs) contribute[2] to this diffractive enhancement. Detailed studies of the 2- and the 4-prong events show that their single diffractive contributions to the low mass peak are 2.05 ± 0.22 mb and 2.38 ± 0.16 mb, respectively.[3, 4] In the 4-prong events, 25% of the low mass peak was found to come from the $pp\pi^+\pi^-$ final state, with the remainder consisting of states with 3- or more pions. From an analysis of the missing mass spectrum, the 6-prong events were estimated to contribute 0.52 ± 0.18 mb to the total diffractive cross section.[2] All these numbers are quoted for both center-of-mass (c.m.) hemispheres.

In this paper we report on our study of the complete 6-prong events and on their contribution to the low mass peak observed in reaction (1). Previously,[2] only the slow proton was measured and no information was obtained about the individual make-up of the system X. The new results come from measurements of all outgoing tracks for those 6-prong events, in a given fiducial region, which had a proton with laboratory momentum less than 1.4 GeV/c. Our selected data sample consists of 442 events corresponding to a microbarn equivalent of 6.06 μb/event.

We first present the evidence for diffractive dissociation of the beam particle. Fig. 1(a) shows the square of the missing mass, MM^2, of the system recoiling from the slow proton. In Fig. 1(b-f) we show this MM^2

distribution subdivided according to the number of charged particles in the forward c.m. hemisphere. We refer to events with i charged particles in the forward c.m. hemisphere and j charged in the backward c.m. hemisphere as "(i, j)" events. We note that the events with low MM^2 are almost all of the (5, 1) type, with a small contribution from the (4, 2) events.

To continue the analysis, we consider the particle distributions in the ordered rapidity chain. We use the pseudo-rapidity variable

$$\eta = \ln(\tan\theta/2) \quad , \tag{2}$$

where θ is the laboratory production angle for an outgoing particle. For those events in which the beam particle diffractively dissociates, we expect the recoiling target proton to be well separated from the remaining particles in the ordered rapidity chain as shown in Fig. 2.

In our study of the diffractive process in the 4-prong events, we used the technique of rapidity gap analysis and a minimum rapidity gap $\Delta\eta = 2.5$ was found appropriate to define diffraction. Fig. 3(a) shows the MM^2 distribution for the 6-prong events which have a proton on the left-hand end of the rapidity chain of Fig. 2 and for which the largest η gap is also the first gap. Comparing this to Fig. 1(a), we note that almost all the events with $MM^2 < 40$ GeV^2 appear in Fig. 3. The cross-hatched events have the first gap greater than 2.5 units. For these events, the average η of the five particles is 4.6 units and the average spread in η for the five-particle cluster is 2.3 units. Using the same definition as was previously used for the 4-prong events, we find 64 events with $\Delta\eta > 2.5$ units and $MM^2 < 40$ GeV^2. This corresponds to a single diffractive cross section of 0.88 ± 0.12 mb,[5] which is somewhat larger than the diffractive cross section of 0.52 ± 0.18 mb estimated from an analysis of the MM^2 distribution only.[2] Our definition of diffraction

involves no background subtraction and does allow some pions to be in the backward hemisphere.

To estimate the contribution to the diffractive peak from the reaction

$$pp \rightarrow pp\pi^+\pi^+\pi^-\pi^- \quad , \tag{3}$$

we have fitted the 6-prong events with the kinematic fitting program SQUAW and looked for 3- or 4-constraint fits. Since we are interested in fits for which a proton is the fastest particle in the lab frame, we accepted only those fits for which the fast forward proton had laboratory momentum > 150 GeV/c. Our previous analyses[3, 4] of the inclusive distribution in Feynman x ($x = P_{||}/2\sqrt{s}$) for positive pions show very few events with $|x| > 0.6$, and so we have also required the π^+ laboratory momentum to be < 110 GeV/c (corresponding to $x < 0.6$). In Fig. 3(b) we show the distribution in MM^2 from the slow proton for the events with accepted fits to reaction (3), and for which the largest η gap is the first gap. Almost all events have $MM^2 < 20$ GeV^2 and correspond to a cross section of 0.18 ± 0.07 mb, 20% of the total 6-prong diffractive cross section.[6]

Fig. 3(c) shows those diffractive events which do not have accepted fits to reaction (3). Note that the peak is at a higher value of MM^2 than for the events assigned to reaction (3). This agrees with earlier observations that the diffractive peak moves up in MM^2 as the number of constituent particles increases.[4] The results for the various topologies are compared in Table I and illustrated in Fig. 4, which shows the diffractive peak for various topologies, both with and without missing neutrals.

In a companion study,[7] we have determined the characteristics of inclusive Δ^{++} production. One interesting question is the extent to which the

Δ^{++} results from the decay of a higher mass diffractively-produced state. Since the Δ^{++} inclusive cross section is about equal to the diffractive cross section for the 6-prong events, this topology is important for a study of the connection between diffraction and Δ^{++} production. To investigate this question, we have chosen the events that are symmetric in the c.m. system to the (5, 1) events of Fig. 1(b). In Fig. 1 we see that there are only 41 (1, 5) events present, whereas we observe 85 (5, 1) events. After making a 15% correction for events with two fast protons[5] ($P_{Lab} > 1.4$ GeV/c), this implies that about 35% of the (5, 1) events contain a neutron in the final state.

Fig. 5(a) shows the $p\pi^+$ mass distribution for the (1, 5) events in which the target has diffracted. A clear peak corresponding to Δ^{++} production is observed. This peak of 18 events above background gives a cross section of 0.22 ± 0.06 mb, which may be compared to the inclusive 6-prong Δ^{++} cross section of 0.80 ± 0.10 mb.[7] Thus, there is only about a 25% overlap between diffraction and Δ^{++} production for the 6-prong topology. In Fig. 5(b) the diffractive events also show an enhancement in the Δ^{o} region, but the small number of events and the uncertainty in the background do not allow us to make a quantitative estimate of the Δ^{o} cross section.

We have also studied double diffraction dissociation $pp \rightarrow N^*N^*$, where the symbol N^* is used here to refer to the low-mass enhancement which decays into three charged particles (with or without neutrals). The signal for this reaction is shown in Fig. 6 as a correlated low mass enhancement, both in the mass of slow proton, positive and negative pion system, and in the missing mass to this system. From the six combinations that are candidates for $p\pi^+\pi^-$, we have selected one per event. To be selected, the combination must have

mass squared less than 40 GeV^2 and momentum transfer from the target proton lower than in any other such combination. To estimate the background, we have repeated the same selection procedure for the non-diffractive combinations $p\pi^-\pi^-$. The $p\pi^+\pi^-$ and $p\pi^-\pi^-$ mass distributions are shown in Fig. 7(a) as the open and cross-hatched histograms, respectively. There is a clear excess of the signal ($p\pi^+\pi^-$) over the background ($p\pi^-\pi^-$). Fig. 7(b) shows the MM^2 distribution from the events of Fig. 7(a) where now the open histogram corresponds to the missing mass recoiling off the $p\pi^+\pi^-$ system of Fig. 7(a) and the cross-hatched histogram to that recoiling off the $p\pi^-\pi^-$ system. Since we are interested in the shape of the background to the MM^2 distribution, we have area-renormalized the cross-hatched histogram to the open histogram in Fig. 7(b). Although there is an excess at low MM^2 in Fig. 7(b), the large backgrounds and unknown correlations between the signal and background in Fig. 7(a) and (b) only allow us to establish an upper limit for double diffraction. From Fig. 7(b), we obtained $\sigma_{DD} \leq 0.38 \pm 0.12$ mb.[8]

References

1. See, for example, J. Whitmore, Physics Reports 10C, 273 (1974) and Physics Reports 27C, 187 (1976).

2. S. J. Barish et al., Phys. Rev. Letters 31, 1080 (1973).

3. S. J. Barish et al., Phys. Rev. D9, 1171 (1974).

4. M. Derrick et al., Phys. Rev. D9, 1215 (1974) and Phys. Rev. D3, 1853 (1974).

5. A 15% correction results from requiring symmetry in the c.m. system. In the $pp\pi^+\pi^+\pi^-\pi^-$ events, we find 30% fewer slow (target-associated)

protons than fast (beam-associated) protons. This is due to the cut-off at a laboratory momentum of 1.4 GeV/c that was applied to select the slow protons. We apply the same 15% correction to all 6-prong events.

6. Following the analysis described in Ref. 4 for the reaction $pp \to pp\pi^+\pi^-$, we have subtracted a background of $(20 \pm 7)\%$ to account for events which actually have one or more missing neutrals.

7. S. J. Barish et al., Phys. Rev. D12, 1260 (1975).

8. In a study of 6-prong events at 300 GeV/c, Firestone et al., Phys. Rev. D12, 15 (1975) report a $\sigma_{DD} = 0.12 \pm 0.05$ mb.

Table I

Properties of the Low Mass Diffractive Enhancement in $pp \to pX$ at 205 GeV/c

	Composition of Final State	Approximate MM^2 Peak Position (GeV^2)	Cross Section (mb) (Both Hemispheres)
2-prong inelastic	$N + \geq 1\pi$	2	2.04 ± 0.22
4-prong 3C-4C fits	$p\pi^+\pi^-$	4.5	0.64 ± 0.14
remaining 4-prongs	$N + \geq 3\pi$	10	1.92 ± 0.16
6-prongs 3C-4C fits	$p\pi^+\pi^+\pi^-\pi^-$	15	0.18 ± 0.07
remaining 6-prongs	$N + \geq 5\pi$	35	0.70 ± 0.11

Figure Captions

Fig. 1 Missing mass squared (MM^2) distributions for the system recoiling from the slow proton in 6-prong events: (a) all events, (b) 85 events with 5 particles in the forward c.m. hemisphere, (c) 108 events with 4 particles in the forward c.m. hemisphere, (d) 131 events with 3 particles in the forward c.m. hemisphere, (e) 77 events with 2 particles in the forward c.m. hemisphere, and (f) 41 events with 1 particle in the forward c.m. hemisphere.

Fig. 2 Configuration of particles in $\eta = \ln(\tan \theta/2)$ for a beam diffraction dissociation in a six-prong event.

Fig. 3 Missing mass squared (MM^2) recoiling off the slow proton for those events with the proton on the end of the ordered rapidity chain and for which the largest rapidity gap is the one separating the proton from its nearest neighbor: (a) all 6-prong events, (b) events giving acceptable fits to the reaction $pp \rightarrow pp\pi^+\pi^+\pi^-\pi^-$, (c) remaining events, i.e., the difference between (a) and (b). The cross-hatched events correspond to those for which the first gap is greater than 2.5 units.

Fig. 4 Missing mass squared (MM^2) distribution for the system recoiling from the slow proton for (a) the inelastic 2-prong events, (b) the (3, 1) 4-prong events fitting $pp \rightarrow pp\pi^+\pi^-$, (c) the remaining 4-prong events, (d) the (5, 1) 6-prong events fitting $pp \rightarrow pp\pi^+\pi^+\pi^-\pi^-$, (e) remaining 6-prong events.

Fig. 5 (a) Effective mass of slow proton plus π^+ for the (1, 5) events; there are two entries per event. A Δ^{++} signal is evident. (b) Effective mass of slow proton plus π^- for the (1, 5) events.

Fig. 6 Scatter plot of $M^2(p\pi^+\pi^-)$ vs. the missing mass squared. There is one entry per event selected as that $p\pi^+\pi^-$ combination with $M^2(p\pi^+\pi^-) < 40\ GeV^2$ and the lowest momentum transfer from the target proton.

Fig. 7 (a) Distribution in $M(p\pi^+\pi^-)$, one combination per event with $M^2(p\pi^+\pi^-) < 40\ GeV^2$, and the combination with lowest momentum transfer chosen. The cross-hatched events represent the background $p\pi^-\pi^-$ combinations. (b) Distribution in the square of the missing mass recoiling against the selected $p\pi^+\pi^-$ system. The cross-hatched events represent the background using the system recoiling against the $p\pi^-\pi^-$ combinations.

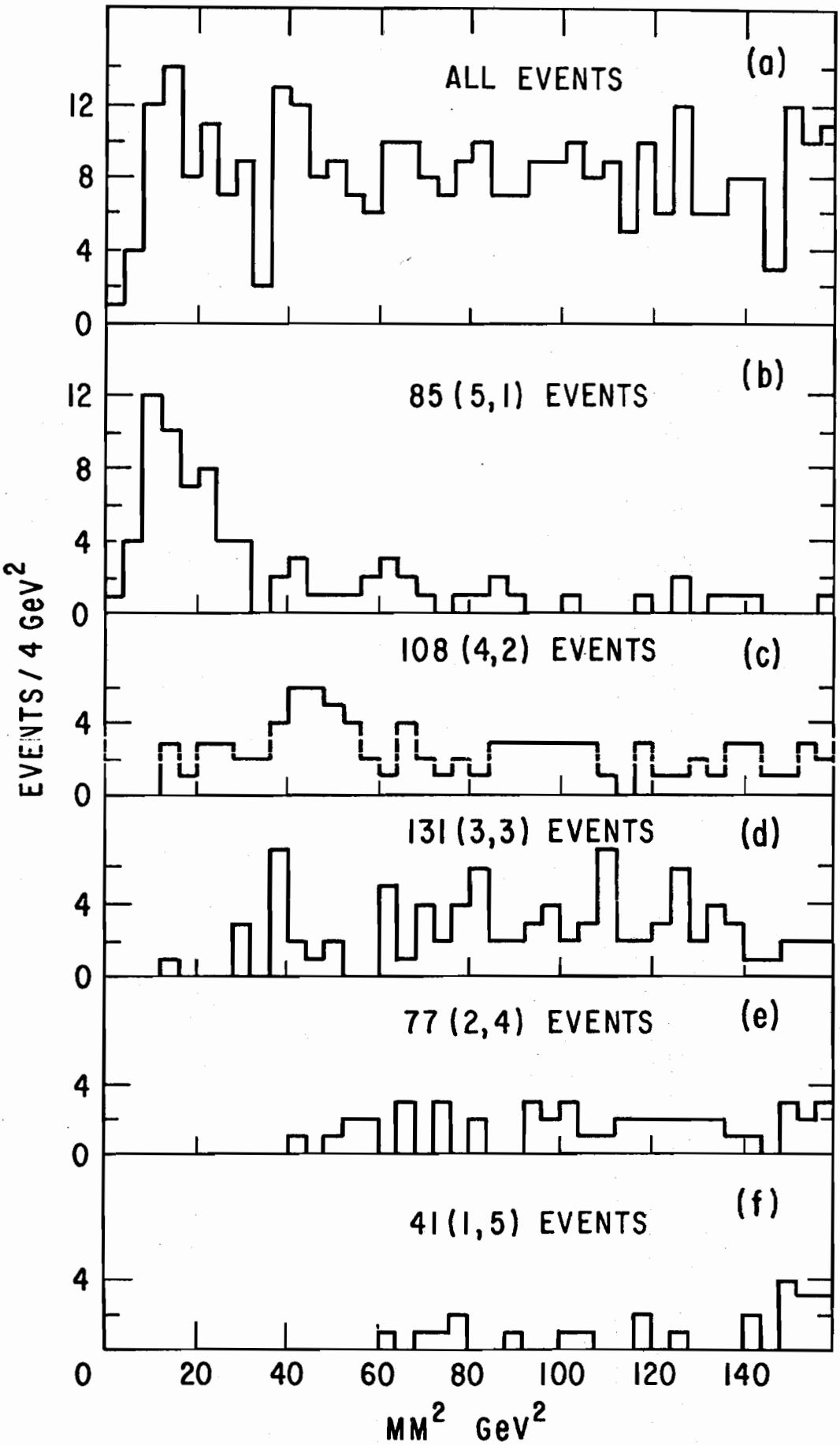
ALL EVENTS
(a)
85 (5,1) EVENTS
(b)
108 (4,2) EVENTS
(c)
131 (3,3) EVENTS
(d)
77 (2,4) EVENTS
(e)
41 (1,5) EVENTS
(f)
EVENTS / 4 GeV^2
MM^2 GeV^2
0
4
8
12
20
40
60
80
100
120
140

Fig. 1

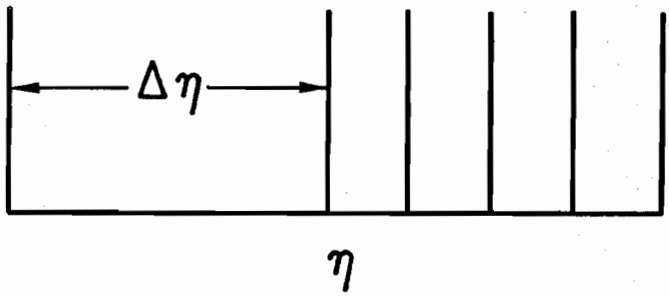

Fig. 2

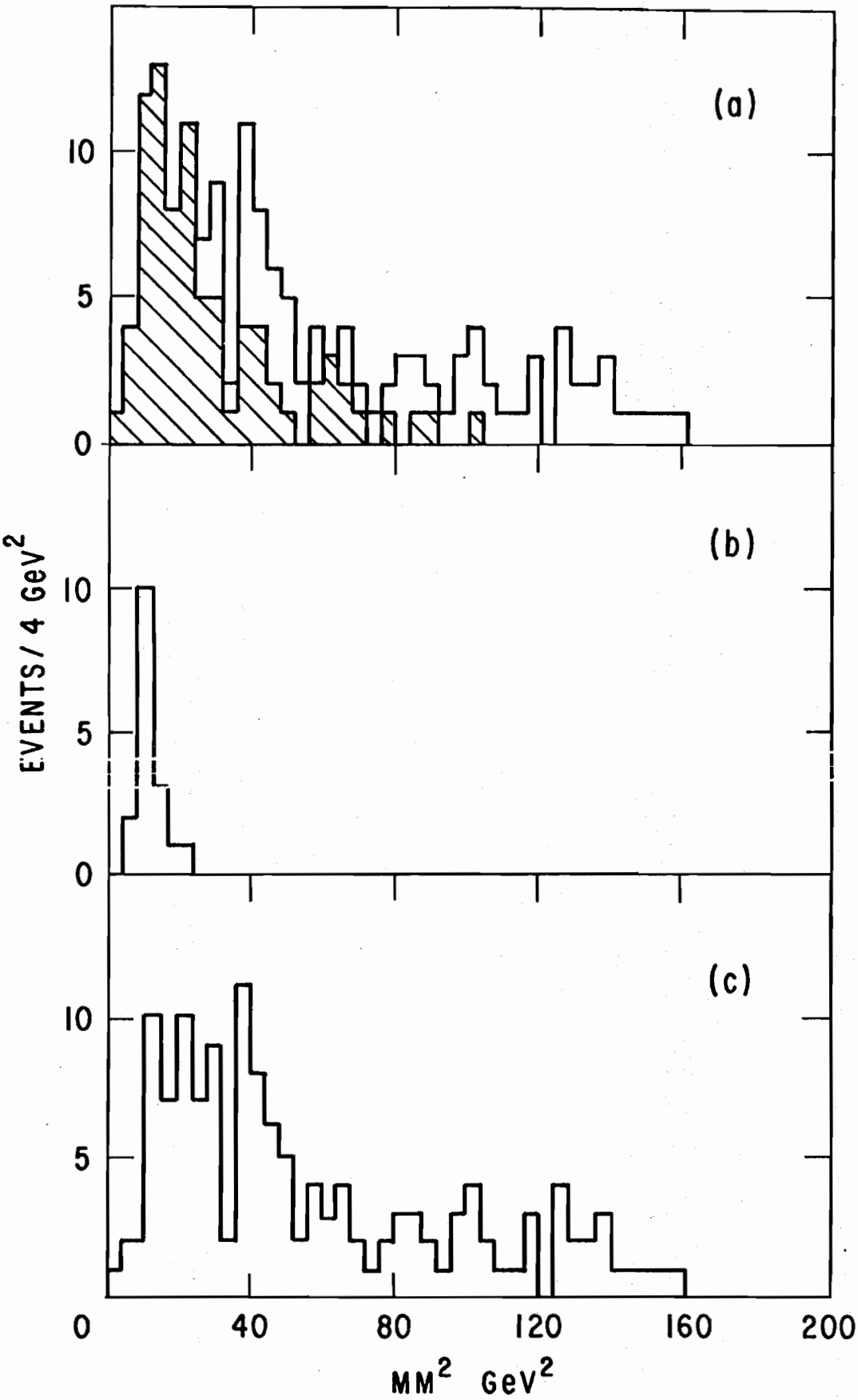

Fig. 3

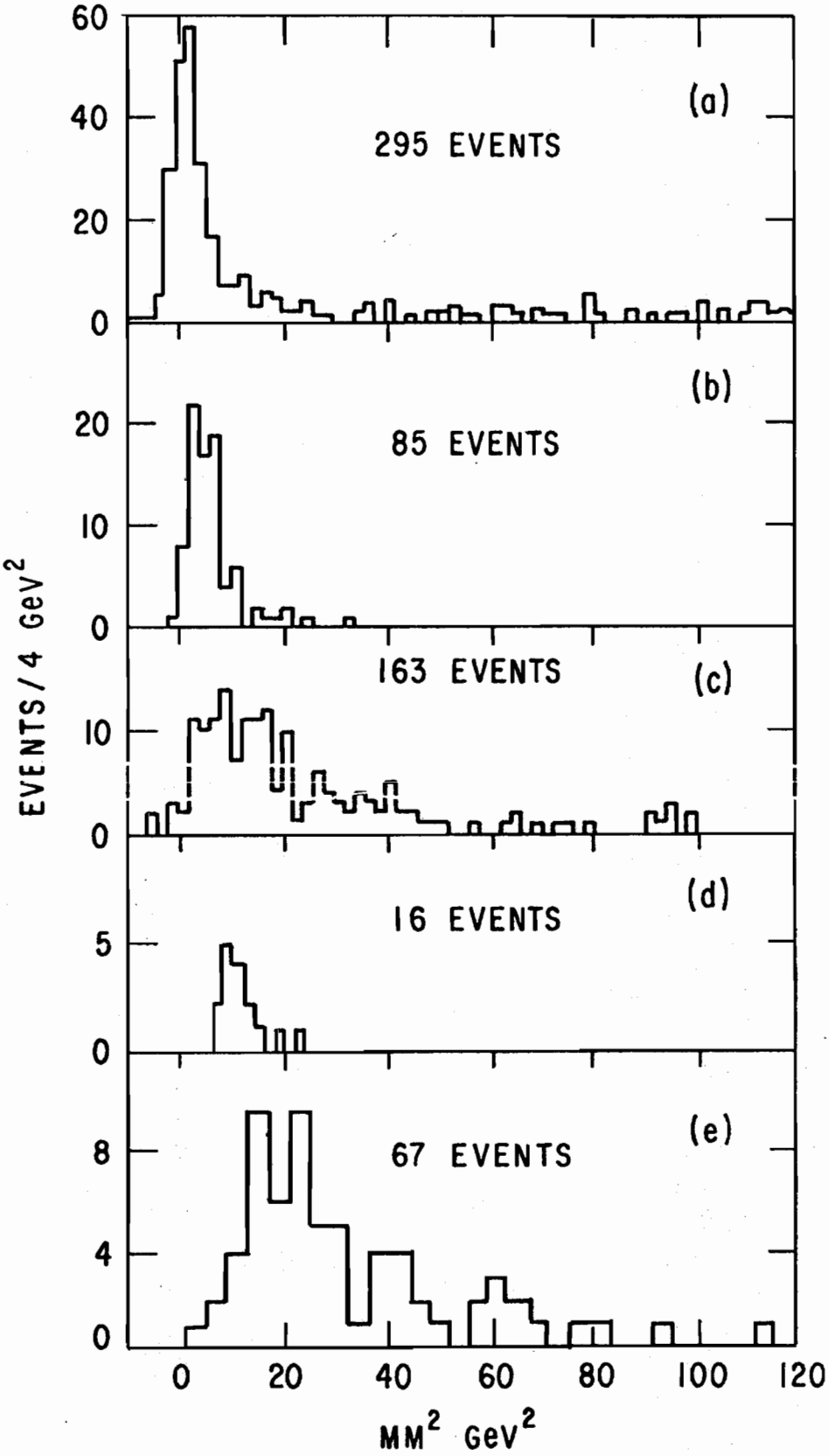
60
40
20
0
(a)
295 EVENTS
20
10
0
(b)
85 EVENTS
10
0
163 EVENTS
(c)
5
0
(d)
16 EVENTS
8
4
0
(e)
67 EVENTS
EVENTS/4 GeV^2
0
20
40
60
80
100
120
MM^2 GeV^2

Fig. 4

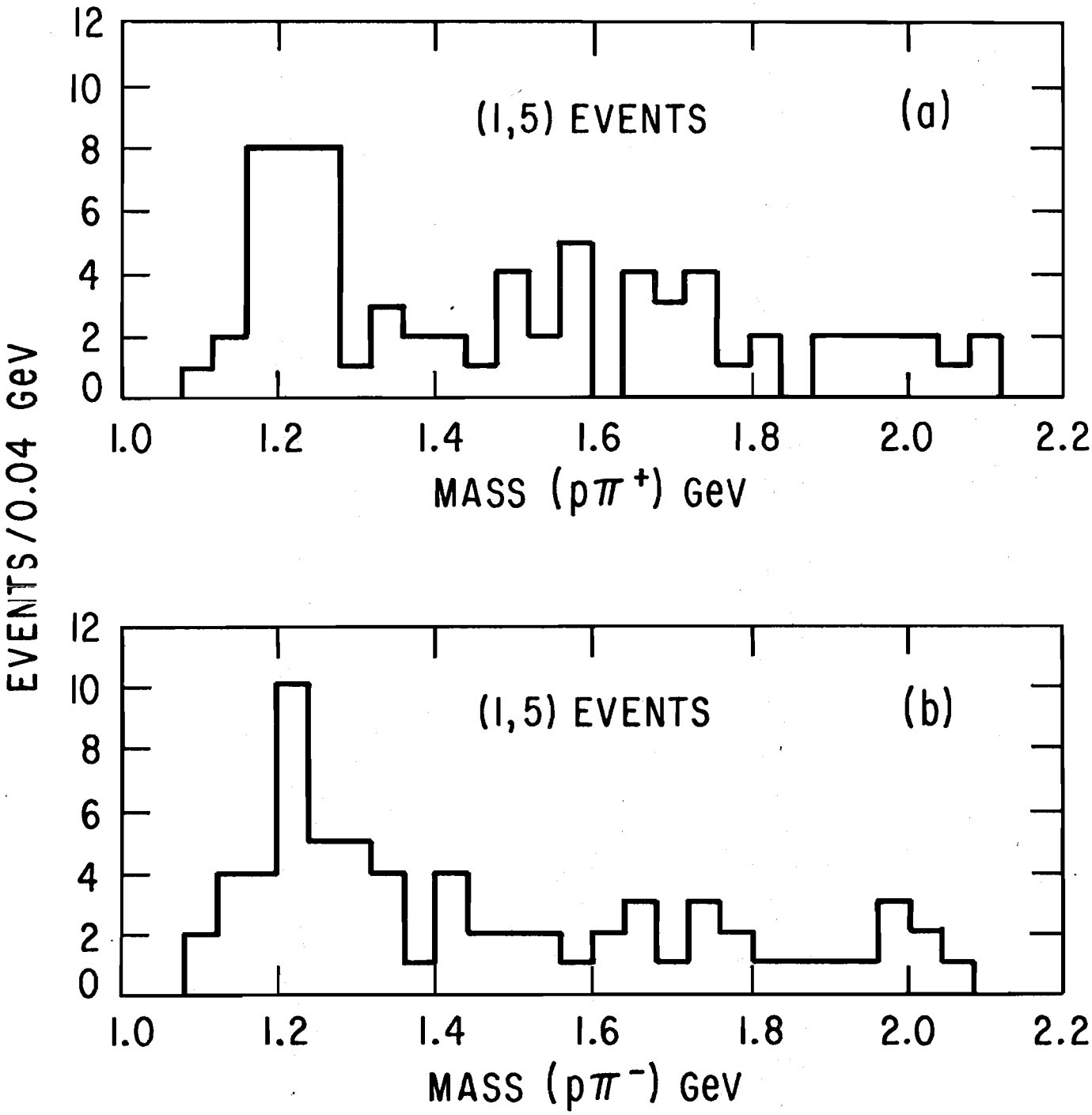
EVENTS/0.04 GeV
(1,5) EVENTS
(a)
MASS ($p\pi^+$) GeV
(1,5) EVENTS
(b)
MASS ($p\pi^-$) GeV
0
2
4
6
8
10
12
1.0
1.2
1.4
1.6
1.8
2.0
2.2

Fig. 5

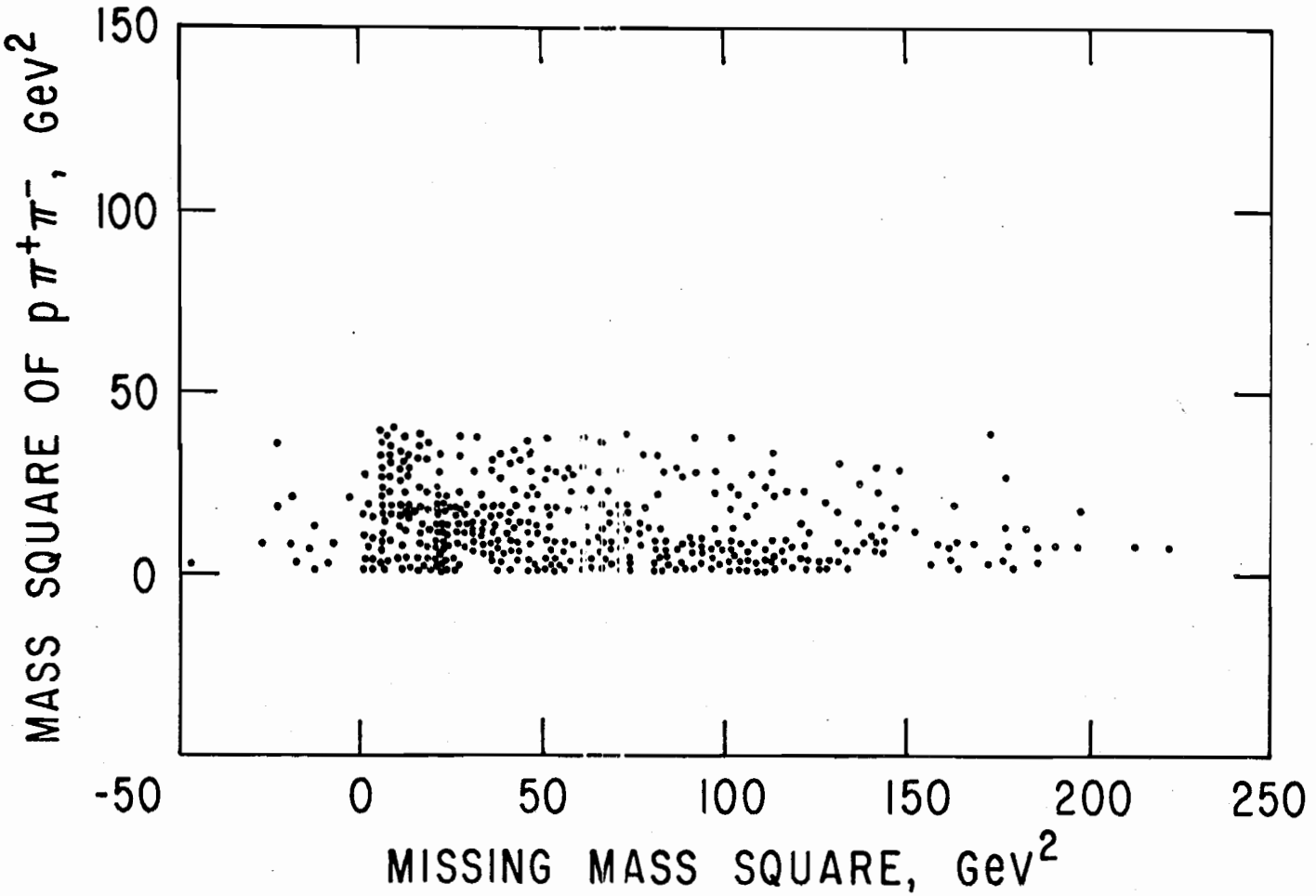
150
100
50
0
-50
0
50
100
150
200
250
MASS SQUARE OF $p\pi^+\pi^-$, GeV^2
MISSING MASS SQUARE, GeV^2

Fig. 6

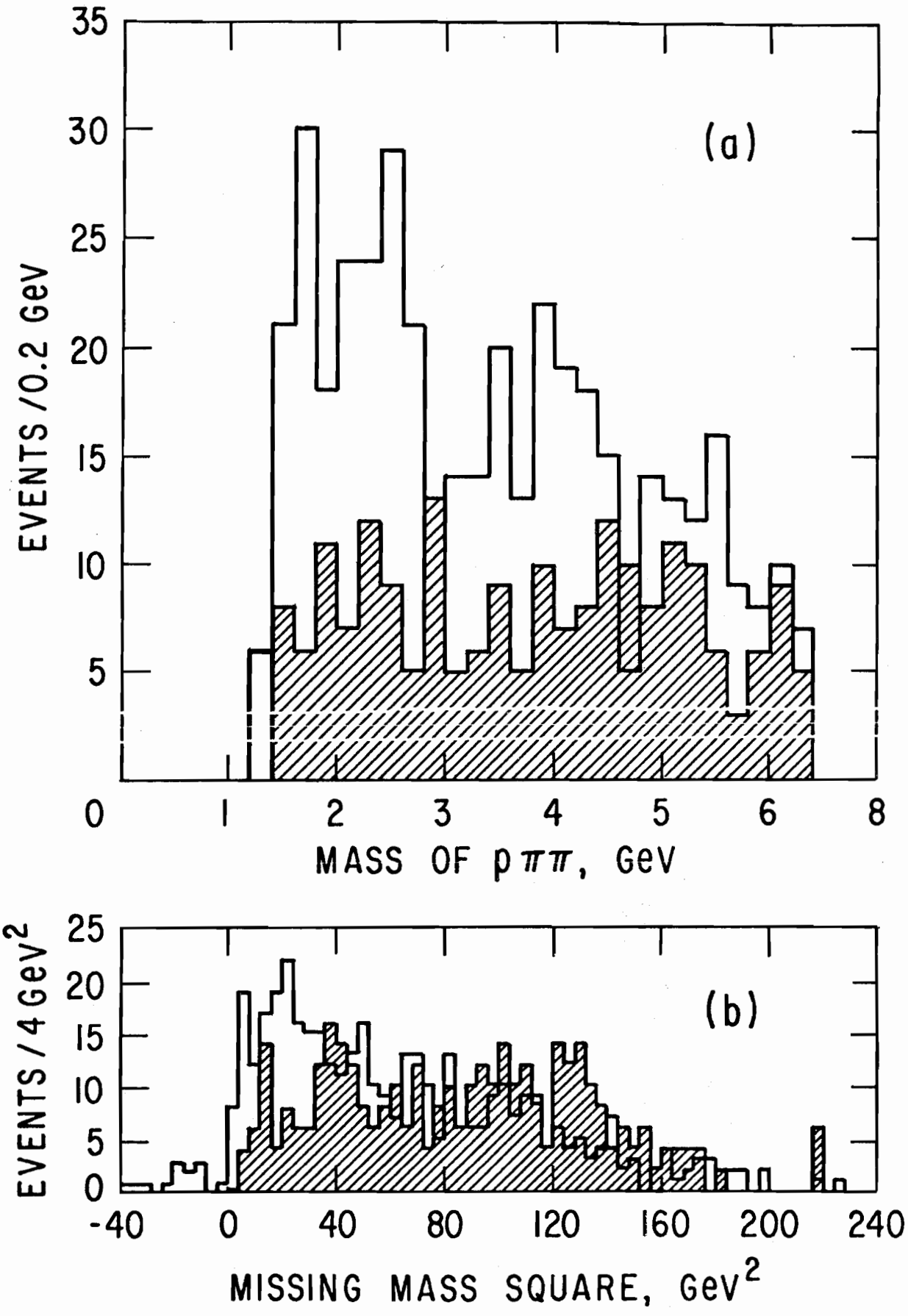
(a)
EVENTS /0.2 GeV
MASS OF pππ, GeV
(b)
EVENTS /4 GeV²
MISSING MASS SQUARE, GeV²

Fig. 7